

PAPER • OPEN ACCESS

Steel skin – SMC laminate structures for lightweight automotive manufacturing

To cite this article: Luca Quagliato *et al* 2017 *J. Phys.: Conf. Ser.* **896** 012086

View the [article online](#) for updates and enhancements.

Related content

- [Impact resistance of metal skin-carbon fiber reinforced polymer laminate structures for the production of lightweight vehicles body frame](#)
Luca Quagliato, Kim Dongwook, Jang Changsoon et al.
- [The aluminizing in powder technology of AISI 304 steel](#)
D B Bitanu, D G Gluc, D C Achiei et al.
- [Corrosion resistance of the AISI 304, 316 and 321 stainless steel surfaces modified by laser](#)
B. Szubzda, A. Antoczak, P. Kozio et al.

Steel skin – SMC laminate structures for lightweight automotive manufacturing

Luca Quagliato¹, Changsoon Jang², Mohanraj Murugesan² and Naksoo Kim²

¹ Department of Management and Engineering, University of Padua, Vicenza, 36100, Italy

² Department of Mechanical Engineering, Sogang University, Seoul, 04107, Korea

E-mail: nskim@sogang.ac.kr

Abstract. In the present research work an innovative material, made of steel skin and sheet molding compound core, is presented and is aimed to be utilized for the production of automotive body frames. For a precise description of the laminate structure, the material properties of all the components, including the adhesive utilized as an interlayer, have been carried out, along with the simple tension test of the composite material. The result have shown that the proposed laminate structure has a specific yield strength 114% higher than 6061 T6 aluminum, 34% higher than 7075 T6 aluminum, 186% higher than AISI 304 stainless steel (30HRC) and 42% than SK5 high-strength steel (52HRC), showing its reliability and convenience for the realization of automotive components. After calibrating the material properties of the laminate structure, and utilizing as reference the simple tension results of the laminate structure, the derived material properties have been utilized for the simulation of the mechanical behavior of an automotive B-pillar. The results have been compared with those of a standard B-pillar made of steel, showing that the MS-SMC laminate structure manifests load and impact carry capacity comparable with those of high strength steel, while granting, at least, an 11% weight reduction.

1. Introduction

In the automotive industry, the requirements for CO₂ emission reduction is becoming an impelling issue which needs to be answered, either by improving the performances of the engine or by reducing the weight of the vehicle. Being the combustion engine a more than one-century old technology, the small improvements of the recent years seems not to properly answer the call for a substantial increasing of the vehicle efficiency. Concerning the latter, innovative a smart material can be utilized to replace the standard one, i.e. steel, and, in this way, reduce the weight of the vehicle, thus increase the overall efficiency, while reducing the CO₂ emissions. This is the case of laminate structures made of steel skin and sheet molding compound core, linked together by a thin layer of adhesive, which increases the stiffness of the composite. In the literature, several contributions dealt with the behavior characterization and possible application of hybrid structures made of different layers of polymer, both fiber reinforced and not, and metal, as follows. Kim et al. [1] utilized both the Hill's (1948) and Barlat (2000) yield functions to account for the planar anisotropy of laminate structures made of AA5152 aluminum skin and polypropylene core, deriving the FLD (forming limit diagram) of the laminate structure. Same concerning aluminum skin laminate structures, Liu et al. [2] developed the forming limit diagram for the AA5052/polyethylene/AA5052 structures, showing the importance of the



thickness of the polymeric core in the formability of the hybrid material. In addition to that, Weiss et al. [3] studied the influence of the forming temperature on the material properties of metal/polymer laminates made of AA5152 aluminum and polypropylene core. Although the influence of the forming temperature has shown to have a marginal effect on the formability of the laminate structure, it has a not negligible effect on the spring back and higher forming temperature tends to reduce the spring back effect. Concerning the utilization of steel for the realization of the skin of the laminate structure, Carraddò et al. [4] studied the potential formability application of sandwich structures with steel, or aluminum, skins and with reinforced polymer core, comparing the formability results with those of the materials normally available in the market. In addition to that, both Harhash et al. [5] and Sokolova et al. [6] studied the mechanical properties and forming behavior of steel-polymer-steel composite structures. In the first contribution, the influence of the percentage of reinforcement in the polymer influences both the strain distribution and the fracture mode. In the latter one, the deep-drawing formability of 316L-PP-PE-316L (stainless steel skin and double polymer core) has been characterized, highlighting how both core thickness and geometry of the punch highly influence the formability. In the laminate structures made of different materials, such as the case of steel and carbon fiber reinforced polymers, the joining strength between different layers is of key importance for the distribution of the load, thus for the overall load carrying capacity. Ochoa-Putman [7] analysis the chemical conditions those allow enhancing the joining strength between polymers and metals, underlining how an appropriate surface treatment can be helpful in increasing the adhesion. In addition to that, in the work of Xia et al. [8], the parameters those influences the joining strength between steel and fiber-reinforced polymers (FRP) have been defined, leading to the development of a bond-slip for the FRP-to-steel interfaces. Concerning the possible additional mechanical anchoring between metal and polymer, in order to enhance the joining strength, Kim et al. [9] proved that the joining strength can be increased by micro-pattern on the metal surface, in order to increase the total work to fracture.

Concerning the fracture modes those can arise when a metal-polymer-metal is subjected to loads, He et al. [10] studied the influence of utilizing linear or non-linear behavior adhesive to bond together metal and polymer, proposing a bond-slip failure for both possibilities, concluding that the failure depends on the properties of the adhesive, regardless the failure is cohesive or delamination. Moreover, in a recent work of Lauter et al. [11], the possibility of increasing the crashworthiness properties of standard steel by applying local carbon fiber reinforced multi-directional pre-pregs has been studied, concluding that this hybrid kind of materials can be successfully be used to increase the impact resistance of materials, while granting a considerable reduction of the weight.

In the present research work the mechanical properties of the components of the laminate structure, namely the steel skin, the adhesive and the sheet molding compound core, are derived from laboratory experiments. Afterward, the material data are utilized to set up a numerical simulation in ANSYS to calibrate the material properties. In order to show the feasibility of the application of the proposed material for the realization of automotive, but not only, body frame, the case of an automotive B-pillar has been taken into consideration and an impact test simulation has been implemented. The comparison between the B-pillar realized by means of the laminate structure and that made of high strength steel show a comparable stress field while granting a remarkable weight reduction.

2. Material model and characterization

The laminate structure proposed in this research paper are composed of three different components, SK5 (DIN 17350) steel skins, sheet molding compound (SMC) core and two thin adhesive layers of adhesive between the previously cited two materials, in order to enhance the cohesion of the structure.

In all the experiments described in the present research work, only one typology of steel and of SMC have been utilized whereas three different adhesives, all epoxy based, have been tested. From the results of the shear strength test, the adhesives which have shown to have good yield strengths have been utilized for the manufacturing of the laminate simple tension test specimens. In order to properly describe the combined behavior of the laminate structure, the interaction between the different layers

should be firstly clarified. In the laminate structure, Figure 1(a), five different layers can be identified, each one of them with an own stiffness and resistance cross-section. If the load is applied along the normal direction of the cross-section of the laminate, all the plies will withstand the same elongation, hence the strain results in $\varepsilon_S = \varepsilon_{AD} = \varepsilon_{SMC}$, while the stress shall be different, according to the cross-section of each layer. When the laminate SS-SMC material undergoes elastic deformations, its stiffness will be a combination of cross-sections area and Young's modulus of its components, namely of the stiffness of steel, adhesive and SMC layers.

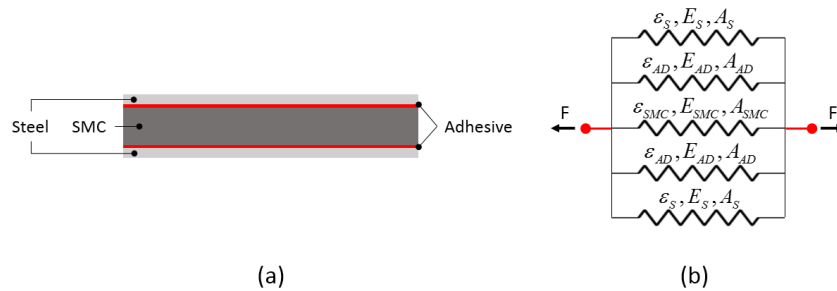


Figure 1. (a) Schematic of the layup of the SS-SMC and (b) equivalent stiffness model

The resulting Young's modulus can be calculated according to the following Eq. (1) and the analytical calculation will be afterward compared with the results of the material characterization.

$$E = \frac{2E_S A_S + E_{SMC} A_{SMC} + 2E_{AD} A_{AD}}{2A_S + A_{SMC} + 2A_{AD}} \quad (1)$$

In Eq. (1), E_S , A_S , E_{SMC} , A_{SMC} , E_{AD} , A_{AD} stand for Young's moduli and the cross-sections of steel, SMC and adhesive layers, respectively.

2.1 SK5 steel material properties

The steel utilized for the realization of the skins of the laminate structure is a cold rolled carbon steel, normally utilized in applications where both elasticity and toughness are required. For the characterization of the relevant material properties, room temperature simple tension tests have been conducted utilizing the ASTM E8 standard, whose size are reported in Figure 2(a), along with an image of the real specimen, Figure 2(b). The specimen has been tested at 3 mm/min pulling speed.

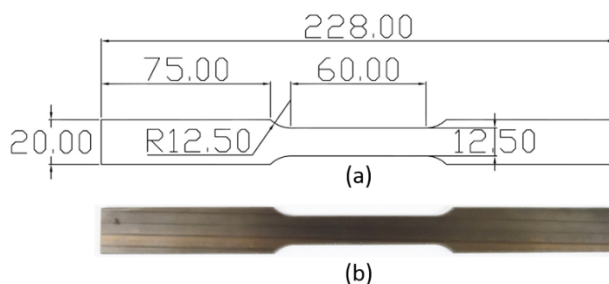


Figure 2. (a) Dimensions and (b) real SK5 steel simple tension specimen

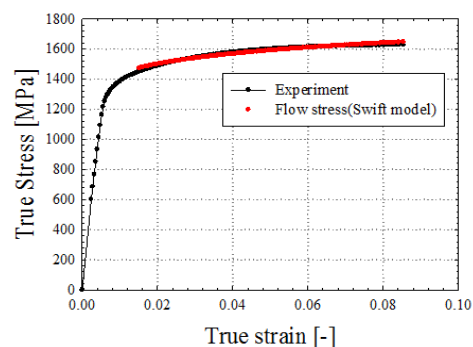


Figure 3. SK5 steel true stress-strain curve and Swift power law fitting

From the results of the tests, Young's modulus has been calculated in 246.3 GPa, whereas the Poisson ratio, required for the proper setting of the numerical simulation, has been assumed to be 0.33, according to the material data sheet. The true stress-strain curve as well as the fitting of the plastic

region, operated utilizing the Swift power law, are reported in following Figure 3. In the Swift power law, the initial strain has been set as $\epsilon_0=0.001$, whereas the model constants have been calculated in $K=2063$ and $n=0.08492$.

2.2 Sheet molding compound (SMC) material properties

The sheet molding compound material utilized for the realization of the core is made of $35\pm 5\%$ chopped carbon fiber, with an average length of 25mm, and for the remaining volume fraction of vinyl-ester resin. The pre-cured SMC is normally manufactured in layers of variable thickness between 2mm and 3mm, those must be compressed and cure, in order to obtain a stiff structure.

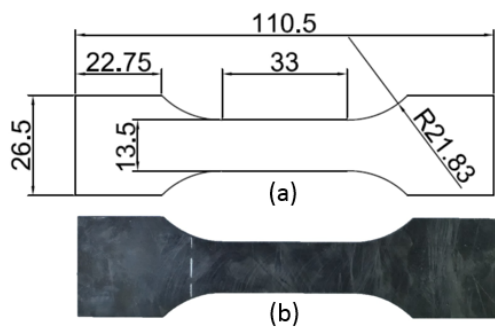


Figure 4. (a) size and (b) real SMC specimen

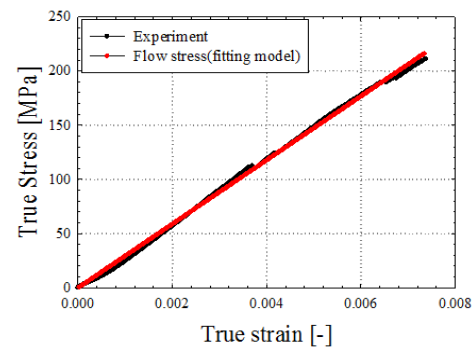


Figure 5. SMC True stress-strain and fitting

For the determination of the material properties of the SMC, an SMC plate has been manufactured by means of the stamping process, stacking together three layers of pre-cured SMC. During the process, a constant force of 5tons has been applied, both top and bottom die have been kept at the constant temperature of 130°C . Moreover, in order to fully cure the SMC, the plate has been kept under pressure for 5 minutes. By means of water jet cutting, the SMC simple tension test specimens, according to the ASTM D638 standard, have been realized and both size and real specimen are shown in Figure 4(a) and Figure 4(b) respectively. The simple tension tests have been conducted at room temperature at the pulling speed of 2 mm/min and the result of both experiment and of the fitting are reported in Figure 5. Since the behavior of the SMC is brittle, the fitting of the experimental data has been operated utilizing a linear function, whose slope and intercept are $m=29450$ and $b=0.7112$.

2.3 Adhesive shear strength characterization

Being the adhesive of key importance for the cohesion of the laminate structure, three different types of epoxy-based resin have been tested, namely: N.F.W. Sealer, EP5055 and ABRO epoxy.

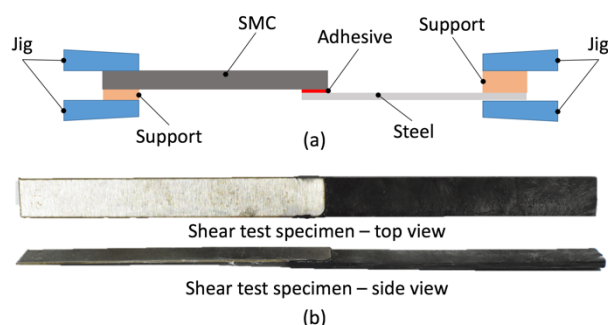


Figure 6. (a) Schematic representation of the shear test and (b) real specimen

In the laminate structure, the adhesive will be normally subjected to a shear load, which will tend to try to separate the steel skin from the SMC core. For this reason, a reasonable way by which to

characterize the mechanical properties of the adhesive is by means of shear strength test, whose schematic representation and real image are shown in Figure 6(a) and Figure 6(b), respectively.

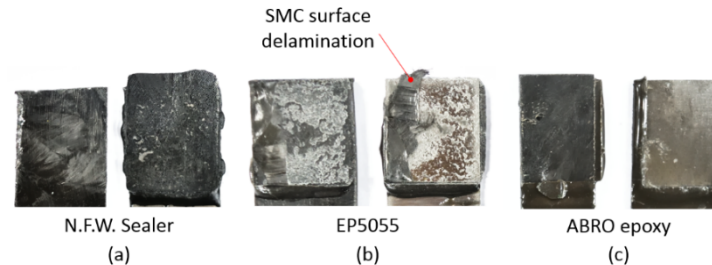


Figure 7. Shear strength test fracture surface for the three tested epoxy-based adhesives

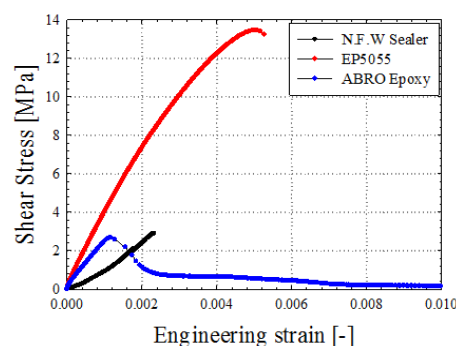


Figure 8. Engineering shear stress – strain for the three tested epoxy-based adhesives

In order to understand the typology of the fracture, detailed pictures have been taken on the fracture surface after the tests and are shown in Figure 7 (a), (b) and (c) for the N.F.W. Sealer, EP5055 and ABRO epoxy, respectively. Based on the results of the fracture surface, the best adhesion is represented by the EP5055 epoxy, whose shear strength has shown to be higher than the adhesion between the SMC layers, as proved by the portion of SMC remaining on the joining surface, on the steel part. Finally, the three engineering shear stress–strain curves, relevant for the three tested adhesives, are reported in Figure 8 where, as also testified by the analysis of the fracture surface, the EP5055 epoxy manifest a shear strength resistance largely greater than the other two adhesives.

2.4 SS-SMC laminate structure characterization

Based on the results of the shear strength test, authors have chosen not to manufacture the laminate specimens with the ABRO epoxy, and to create steel skin – sheet molding compound simple tension test specimens only utilizing the remaining two epoxy-based resins, namely N.F.W. Sealer and EP5055. Both SK5 and SMC have been cut, by means of water jet process, to the specimen size shown in previous Figure 4(a). Afterward, a 0.15 ± 0.05 mm layer of adhesive has been placed between them, according to the scheme shown in Figure 1(a). The two steel skins have a 0.4 mm thickness each one whereas that of the SMC core, due to process intrinsic variations, is 3.5 ± 0.3 mm.

Concerning the specimen realized with the N.F.W. Sealer, the curing of the laminate has been operated applying a 3 kg load, to remove the voids, and inserting the specimens in a chamber at 180°C , for 20 minutes, and letting them to cool down at room temperature for 12 hours. For the manufacturing procedure of the specimen realized with the EP5055 epoxy, the same 3 kg load has been applied for all the curing process, but the specimens have been left to cool cure at room temperature for 4 hours, afterwards placed in a chamber at 100°C for 30 minutes and, in the end, once again left to cool down at room temperature for 12 hours. The SS-SMC specimen is shown in Figure 9 whereas the results, for the specimens made with the two adhesives, are shown in Figure 10. As expectable, also in the simple tension test, the laminate structure realized utilizing the EP5055 as bonding adhesive

between steel and SMC shows a higher true stress value than that realized with the other adhesive, namely the N.F.W. Sealer.



Figure 9. SS-SMC Simple tension test specimen

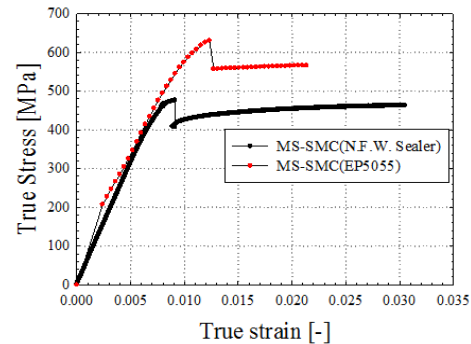


Figure 10. True stress-strain curve and interpolation for the SS-SMC specimens

For this reason, having the combination of SK5-EP5055-SMC shown to be most effective one for load carrying, it will be used for the setting of the following numerical simulation, as well as for the estimation of the specific strength. Moreover, in Figure 10, the abrupt reduction of the stress, followed by a quasi-hardening curve, is due to the widespread fracture of the adhesive between steel and SMC, which makes the load transfer between layers to be suddenly reduced. After that point, the load is carried almost only by the steel, as confirmed by the exponential behavior of the curve, typical of the steel. At failure, steel and SMC break almost together, in the necking region for the steel and with an interlaminar crack in the SMC. In order to show the potentiality of the proposed laminate structure in comparison to standard materials, normally, but not only, utilized for the manufacturing of vehicles, in Table 1, a collection of yield strength and ultimate tensile strength data is reported. The comparison aims to show that the laminate structure, made of steel skin and SMC core, has higher specific yield strength and higher specific ultimate tensile strength than standard materials. The comparison of both specific yield strength and specific ultimate tensile strength shown higher performance for the steel skin – SMC laminate structure than all the standard materials, even in comparison to the high strength steel SK5.

Table 1. Specific strength comparison

Material	Yield Strength [MPa]	UTS [MPa]	Density [kg/dm ³]	Specific Yield Strength [MPa]	Specific UTS [MPa]
AISI 304 Stainless steel (30HRC)	215	505	7.87	27.32	64.17
Al 6061 - T6	276	310	2.80	98.57	110.71
Al 7075 - T6	503	559	2.80	179.64	199.64
SK5 HSS (52HRC)	1350	1522	7.87	171.54	193.40
SS-SMC	630	630	2.95	213.56	213.56

3. Model implementation

The numerical simulation has been implemented in ANSYS and has a double aim: the first one is to calibrate the material properties in the numerical simulation in order to obtain the same behavior of the laboratory experiments. In the second instance, once simulation and numerical simulation of the simple tension test matches in terms of stress-strain behavior, the material will be utilized to in an impact simulation, to test the crashworthiness of the proposed laminate structure, in comparison one with the same geometry, but realized with SK5 steel. In order to check the influence of two different

modeling strategy, two simulations have been set up. In the first one, the SS-SMC material behavior has been described as an isotropic material, with the properties resulting from the material characterization described in previous section 2.4. In the second one, the behavior of the laminate structure has been described considering different material properties for each layer, as in the real specimen, for a more accurate description of the interaction between the materials. The simulation model, as well as the section of the isotropic and laminate simulations case, are shown in Figure 11.

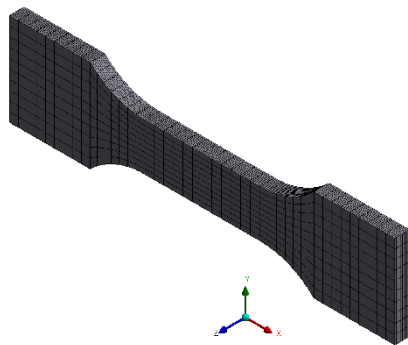


Figure 11. Simple tension test model (ANSYS)

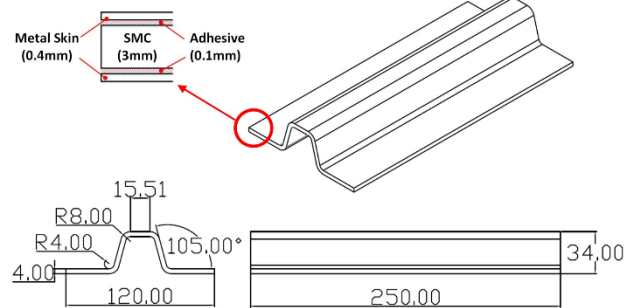


Figure 12. B-pillar dimensions

Concerning the impact test simulation, a simplified automotive B-pillar geometry has been utilized, Figure 12, and the crashworthiness property of the SS-SMC modeled as a laminate structure, and that of the SK5 steel, have been tested utilizing a cylinder shape as impactor and an impact speed of 25m/s.

In both the simple tension test and the impact test simulation the HEX20 element has been utilized, with a mesh skewness factor of 0.47 in the first one and 0.44 in the later one, both in the range where the mesh assures a good calculation of the results.

4. Results and discussion

The results, in terms of von Mises equivalent stress, for the isotropic material simulation are shown in Figure 13, whereas, in Figure 14, the comparison between isotropic material simulation, laminate material simulation, and relevant experiment, for the elastic part of the behavior, are shown. In the elastic region, both the isotropic and laminate material behavior simulations well match with the experimental result but the first one is not able to take into account the failure of the adhesive, as it can the second one, instead. For this reason, in order to better simulate the overall behavior of the laminate structure, in the impact simulation, the laminate behavior has been utilized. Concerning the results of the impact test on the B-pillar shape, the von Mises equivalent stress is shown in Figure 15, for the SS-SMC laminate structure, and in Figure 16, or the SK5 material implementation.

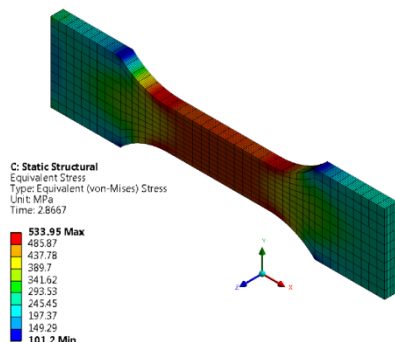


Figure 13. von Mises equivalent stress in the isotropic simple tension test simulation

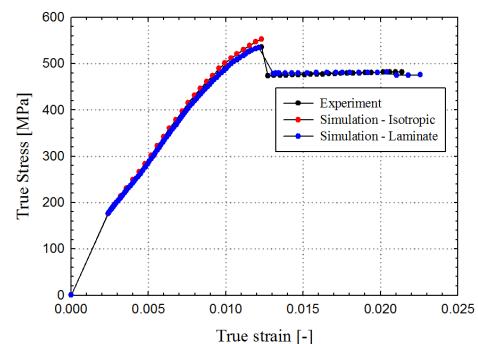


Figure 14. SS-SMC simulation – experiment results comparison

In order to provide a quantitative estimation of the improvement of the crashworthiness property of the SS-SMC laminate structure, in comparison with that of the SK5 steel, the critical strain energy

density, according to the Beltrami formulation equation, have been calculated and results in 3153.5, for the SS-SMC, and in 4826.4, for the SK5 steel. Considering, however, that the density of the steel is 7.87kg/dm^3 whereas that of the laminate structure 2.95 kg/dm^3 , the specific critical strain energy density is calculated in 613.3 for the high strength steel and 1069.0 for the laminate structure. In addition to that, the detailed in Figure 15 and Figure 16 shows that, in the steel made B-pillar, the amount of element deletion due to impact is higher than that in the SS-SMC B-pillar, proving once more the higher impact resistance of the laminate structure in comparison to the SK5 steel.

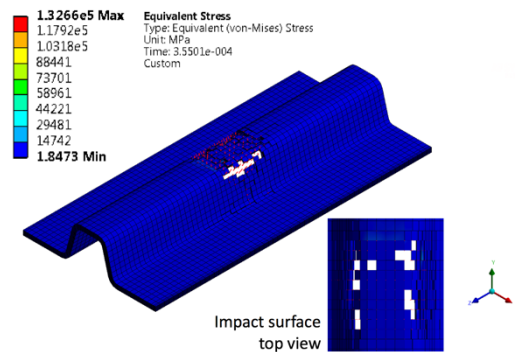


Figure 15. von Mises equivalent stress (ANSYS) for the SK5 HSS steel B-pillar model

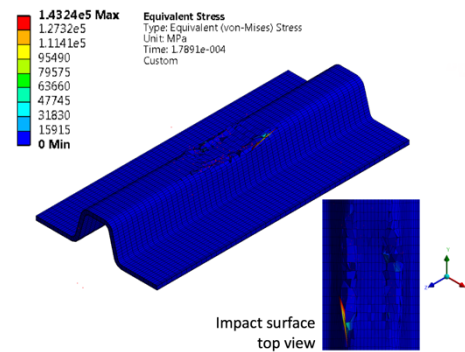


Figure 16. von Mises equivalent stress (ANSYS) for the SS-SMC B-pillar model

5. Conclusion

In the present research work, an innovative material made of steel skin and sheet molding compound core is presented and the relevant material characterization is detailed. Being the adhesive a key component for the proper load transfer between the skins and the core of the composite structure, three different types of bonding have been tested and that which assured the highest bonding strength has been considered for further analysis. In addition to that, the difference of the simulated material behavior in the numerical environment, if an isotropic is taken into account, have been studied and discussed, allowing to conclude that, if the laminate structure is meant to be tested under the yield point, the isotropic assumption is a solution which allows a reduction of computational time, while granting accurate results. If instead, the overall behavior of the material is meant to be properly described, the isotropic assumption should be rejected and a laminate approach should be utilized.

Nevertheless, the calculation of the specific energy density as well as the less amount of element deletion in the SS-SMC simulation than that of the full steel B-pillar, have proved the high crashworthiness properties of the proposed material. Although the results presented in this paper are preliminary, the positive outcomes make this material to be of very interest for all the manufacturing sector where high performance, as well as reduced weight, are driving factors for the product design.

References

- [1] Kim KJ, Kim D, Choi SH, Chung K, Shin KS, Barlat F et al. JR 2003 *J.Mat.Proc.Tech.* **139** 1-7
- [2] Liu J, Liu W, Xue W 2013 *Mat. and Des.* **46** 112-120
- [3] Weiss M, Dingle ME, Rolfe BF and Hodgson PD 2007 *ASME Trans.* **129** 530-537
- [4] Carradò A, Faerber J, Niemeyer S, Ziegmann G and Palkowski H 2011 *Comp. St.* **93** 715-721
- [5] Harhash M, Sokolova O, Carradò A and Palowski H 2014 *Comp. St.* **118** 112-120
- [6] Sokolova OA, Kühn M and Palkowski H 2012 *Arch. Civ. and Mech. Eng.* **12** 105-112
- [7] Ochoa-Putman C and Vaidya UK 2011 *Comp. Part A* **42** 906-915
- [8] Xia SH and Teng JG 2005 *Proc. I. Symp. Bond Behav. FRP Struct.* 411-418
- [9] Kim WS, Yun IH, Lee JJ and Jung HT 2010 *I. J. Adh. & Adh.* **30** 408-417
- [10] He J and Xian G 2016 *Comp. Str.* **153** 12-20
- [11] Lauter C, Niewel J, Zanft B and Tröster T 2015 *15th I. Conf. Exp. Mech.* **2690** 1-7